Distribution and recent variations of supraglacial lakes on dendritic-type glaciers in the Khan Tengri-Tomur Mountains, Central Asia

Liu Qiao [a] *, Christoph Mayer [b], Shiyin Liu [c]

[a] Key Laboratory of Mountain Surface Processes and Ecological Regulation, Institute of Mountain Hazards and Environment, Chinese Academy of Sciences, Chengdu, China
[b] Commission for Geodesy and Glaciology, Bavarian Academy of Sciences and Humanities, Munich, Germany
[c] Stake Key Laboratory of Cryospheric Sciences, Cold and Arid Regions Environmental and Engineering Research Institute, Chinese Academy of Sciences, Lanzhou, China
* Corresponding author: Tel.: +86 013547887225; Email: liuqiao@imde.ac.cn

Abstract

Supraglacial lakes are widely distributed on glaciers in the Tomur-Khan Tengri Tianshan Mountains, Central Asia. Here we mapped the supraglacial lakes on eight typical debris-covered dendritic-type glaciers around the Tomur-Khan Tengri Massif based on 9 Landsat TM/ETM+ images acquired in the summers of 1990 until 2011. With minimum extent of 3600 m^2 for a conservative identification of glacial lakes, we mapped 775 supraglacial lakes and 38 marginal glacial lakes in total. Our results indicate that supraglacial lakes (area > 3600 m^2) in the study region have never developed above an elevation of about 3850 m a.s.l., 800 meter lower than the maximum upper boundary of debris cover (4650 m a.s.l.). The area-elevation distribution shows that lakes predominantly occurred close to the altitude of 3250 m a.s.l., the lower boundary of clean ice. The majority of the supraglacial lakes are found on the Tomur Glacier and the South Inylchek Glacier, two strongly debris-covered dendritic-type glaciers in the region. As for the multi-year variation of lake area, total areas of supraglacial lakes in summer seasons show some variability from 1990 and 2005 but increased noticeably since 2005 (an overall increase of ~39% between 2005 and 2011). The mean area of the mapped lakes reached a maximum in 2010. We found that the extent of supraglacial lakes during August and September is positively correlated to the total summer precipitation (July to September) but negatively to the mean spring air temperature (April to June). Pre-summer air temperature fluctuations likely dominate the evolution processes of glacial drainage, evolving from unconnected to connected systems, which may lead to the drainage of larger supraglacial lakes and results in shrinkage of the total and mean lake area during the summer.

Keywords: Glacier; Remote sensing; Debris-covered glacial; Supraglacial Lake; Khan Tengri-Tomur Tianshan.

this Chinese mean 'deleting'

删除的内容: The existence and development of supraglacial lakes play an important role in the ice melting processes and also in the storage and release of glacial melt water.

删除的内容: of

删除的内容: peaks

删除的内容: a lower area limit

删除的内容: beyond

删除的内容: s are

删除的内容: where the clean ice simultaneously disappears

删除的内容: the summer total and mean

删除的内容: between

删除的内容: and 2011

删除的内容: area

删除的内容: in summer

删除的内容: correlated

删除的内容: have a stronger impact on the different

1 Introduction

Glaciers act as natural water reservoirs because they store water as snow and ice in cold seasons and gradually release it by melting during the warm seasons. Shorter time scales (diurnal or seasonal) changes of glacial runoff display periodic fluctuations and show more remarkable variations (Jansson et al., 2003) than that of longer time scales (interannual or decadal). Seasonal and diurnal glacial runoff fluctuation reflects variations in atmospheric air temperatures and therefore the pattern of ablation on a glacier (Hock, 2005). In some cases this fluctuation is interrupted by catastrophic release events, such as glacial lake outburst floods (GLOFs) (Richardson and Reynolds, 2000) and subglacial floods (Jökulhlaups) (Roberts, 2005), etc. Such uncertainty of glacial melt water release results from the fact that glaciers act as a porous-medium by storing liquid water and releasing it abruptly and stochastically through a changeable englacial and subglacial drainage system (Campbell and Rasmussen, 1973). Liquid water, supplied by melt or rainfall, can be stored in different kinds of water-accumulating features in a glacier, such as supraglacial lakes (ponds) and streams, crevasses, moulins, subglacial cavities (channels) and lakes, and different kinds of ice or moraine dammed lakes, etc (Cuffey and Paterson, 2010;Fountain and Walder, 1998). However, the location, amounts and release mechanisms of the stored water in glacier drainage system usually remains elusive due to its temporal and spatial variability (Fountain and Walder, 1998).

Among all components of a glacier drainage system, supraglacial ponds and lakes are the easiest to be detected. Although direct observations of supraglacial ponds and lakes (Benn et al., 2000) are still limited, remote sensing have contributed to detect, measure and monitor their spatial and temporal changes in recent years (Gardelle et al., 2011;Salerno et al., 2012;Wessels et al., 2002;Box and Ski, 2007). Supraglacial lakes are commonly found in the lower ablation region of some debris-covered valley glaciers, where glacier ice stagnates (Benn et al., 2012;Reynolds, 2000). Many studies have highlighted the temporal evolution of glacial lakes in the central Himalaya and indicated that most of the current big moraine-dammed or ice-dammed lakes are the consequences of coalesce and growth of supraglacial lakes (Benn et al., 2012;Fujita et al., 2009;Komori, 2008;Sakai et al., 2000;Thompson et al., 2012). These glacial lakes pose a potential for GLOFs and destruction of property and loss of human life in the area downstream (Reynolds, 2000;Bajracharya et al., 2007;Jain et al., 2012;Richardson and Reynolds, 2000). Their existence is also found to enhance the ice ablation rate by ice margin calving processes around ponds and lakes (Sakai et al., 2000;Benn et al., 2012;Sakai et al., 1998). Therefore, investigating the conditions of the supraglacial lakes (ponds) formation and distribution will be a significant contribution to tracing their dynamics and the prediction of their future development (Bolch et al., 2008).

In the central Tianshan region, supraglacial lakes are common on many debris-covered glaciers (Wang et al., 2011). The physical conditions of glaciers in the inner Tianshan region enable the formation of different types of glacial lakes. Research in the region has focused on the moraine dammed Petrov Lake (Jansky et al., 2010;2009) and the ice dammed Lake Merzbacher which is famous for its regular outbursts at least once every summer that has lead to remarkable floods in the downstream valley (Glazirin, 2010;Mayer et al., 2008;Ng and Liu, 2009). However, the supraglacial lakes in this region were seldom considered in scientific investigations, even though they are widely distributed in the glacier ablation zone (Han et al., 2010). Recently, several field observations were carried out to monitor some typical supraglacial lakes on the Koxkar Glacier (Wang et al., 2011). In this study, we investigated the supraglacial lakes on eight large

删除的内容: Variations of glacial runoff are primarily forced by the meteorological conditions, which alter the ice melt rate by changing the energy balance. ... [1]

删除的内容: pattern of diurnal and seasonal discharge

删除的内容: “

删除的内容: ”

删除的内容: Much effort has been invested to study the evolution of glacier drainage systems using several methods, such as dye tracing experiments (Chandler et al., 2013;Nienow et al., 1996;Schuler et al., 2004), analyzing the chemical character of glacial melt water and runoff processes (Anderson et al., 2003), ground penetrating radar investigations (Kulessa et al., 2008), borehole observations (Fudge et al., 2008), etc. ... [2]

删除的内容: measurements

删除的内容: observations

删除的内容: They are also formed, predominantly, in topographic lows and compressive flow regimes in the ablation zone of the Greenland Ice Sheet (Banwell et al., 2012;Bartholomew et al., 2011;Box and Ski, 2007). In the central Himalaya, their existence is found to enhance the ice ablation rate by ice ... [3]

删除的内容: Supraglacial lakes are highly variable in space and time. Their lifetime is unpredictable and in ... [4]

删除的内容: Moraine-dammed, ice-dammed, and supraglacial lakes are widely distributed on and adjacent to ... [5]

删除的内容: Here

删除的内容: the

debris-covered glaciers in the Khan Tengri-Tomur Mountains (KTTM), Central Asia, based on mapping multi-year Landsat image series. The study focuses on the spatial distribution and temporal variations of these lakes under summer conditions during 1990 to 2011 and a furtherly discussion will be emphasized to the formation conditions and consequence dynamic of these lakes.

2 Study Area

The Tomur (Pobeda) Peak, 7439 m above sea level (a.s.l.), and the Khan Tengri Peak, 6995 m a.s.l., are the highest peaks of the Tianshan Mountains, at the Kyrgyzstan-China border, southeast of Lake Issyk-Kul (Figure 1). There are more than 40 peaks exceeding 6000 m a.s.l. in the Khan Tengri-Tomur Knot, which forms the largest glacierized complex in the Tianshan (Shi, 2008). The region is located within the zone of the subtropical west jet stream in June to August, resulting in a summer precipitation maximum and cold and dry winters, and making glaciers summer accumulation type (Aizen et al., 1997). A striking glaciological feature of this region is the existence of many large dendritic valley glaciers with thick debris covers (Figure 2). These glaciers are often classified as Tomur-type glaciers by Chinese glaciologists (Wang et al., 1980). There are 1375 glaciers (509 in China) with a total area of 4093 km^2 in the Khan Tengri-Tomur Mountains (Shi, 2008). Meltwater from these glaciers forms the major source for rivers in the internal drainage basins in Central Asia. Tarim river and Balkhash basin are the notable inland basins in which 45-50% of the surface runoff is from glacial runoff (Aizen et al., 1997).

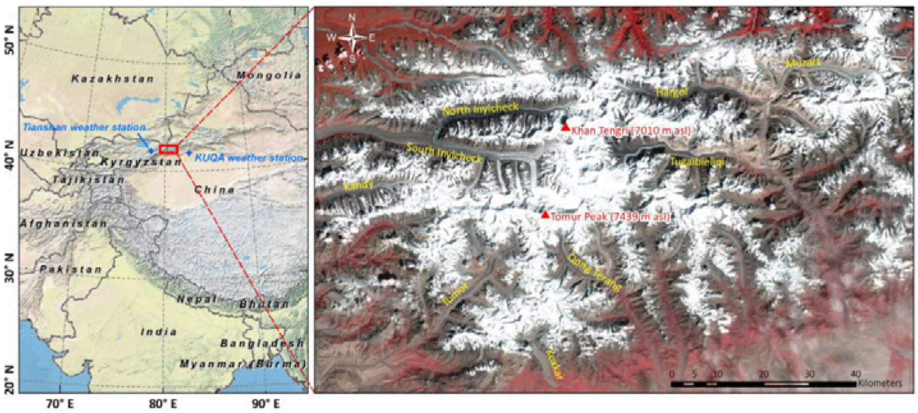

Figure 1 Location map of the Khan Tengri-Tomur Mountains (left) and a Landsat TM image acquired on 24 August 2007 showing the distribution of main glaciers mentioned in the text (right).

删除的内容: of

删除的内容: in

删除的内容: from

删除的内容: A discussion will be emphasized about the formation conditions and consequences the dynamics of these lakes.

删除的内容: located

删除的内容: number of glaciers in this region adds up to 1375 (509 in China)

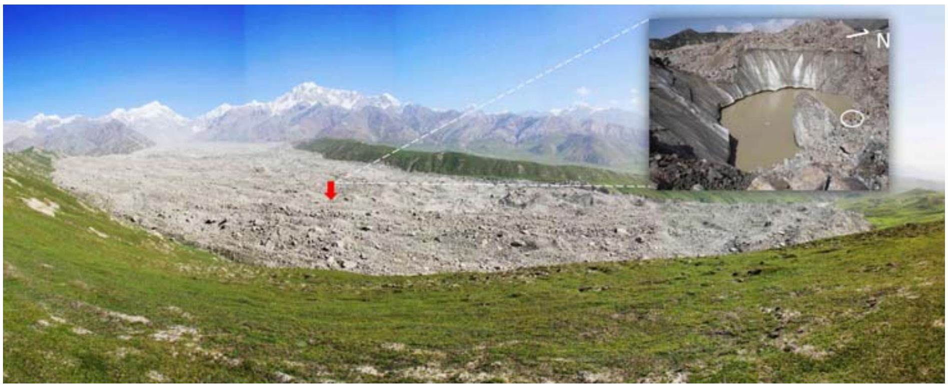

Figure 2 A panoramic view of the lower part of Koxkar Glacier showing the wide flat ablation region covered by extensive debris cover; inset is a supraglacial lake surrounded by ice cliffs, at 3220 m a.s.l. (people in the ellipse for scale). Photographs: Han Haidong and Liu Qiao, during the August 2010 expedition.

There are 7 glaciers with area larger than 100 km^2 in the KTTM region. An impressive characteristic of these glaciers is the extensive supraglacial debris mantle in their ablation zone (Hagg et al., 2008;Han et al., 2006). High amounts of solid precipitation in the firn basins and intensive melting in the ablation areas demonstrate that these glaciers have a high mass turnover (Aizen et al., 1997). High surface velocities in the upper branches indicate a strong erosive and transport capacity (Mayer et al., 2008). Rock falls together with avalanches are probably the main source of the supraglacial debris that is transported downwards by ice flow and finally forms the medial or lateral moraine belts on the surface of the ablation area of the glaciers (Aizen et al., 1997). On the debris-covered glaciers in the KTTM region, the widespread ice cliffs are characterized by higher ablation rate than its surrounding debris covered ice and even higher than on the flat clean ice surface (Han et al., 2010;Mayer et al., 2011;Juen et al., 2013). On the Koxkar Glacier, Han et al. (2010) reported that about 1.13% (0.22 km^2) of the total debris-covered area was occupied by the ice cliffs and melting from ice cliffs produces about 7.3% (1.6×10^6 km^3) of the total melt runoff from the debris-covered area.

3 Data and Methods

For mountain glaciers, supraglacial lakes are generally small and unstable, making detection seasonal variations of supraglacial lakes in the KTTM region difficulty by middle-resolution satellites (in colder seasons mapping is usually influenced by snow cover, lake ice or cloud). Therefore, this study focuses on the multi-year variations of supraglacial lakes for late summer conditions. By searching through the Landsat archives of the United State Geological Survey (USGS), we found nine such Landsat TM or ETM+ images acquired in summer during 1990 and 2011 are of good quality for the change identification of these supraglacial lakes on the eight selected glaciers (see Fig. 1). All images have been orthorectified so that they could be well matched. The spatial resolution (pan-sharpen for Landsat ETM+ spectral bands) and acquisition date of these images are listed in Table 1.

- **删除的内容:** In the Khan Tengri-Tomur Mountains (KTTM), there
- **删除的内容:** exceeding
- **删除的内容:** han Tengri-Tomur Mountains (K
- **删除的内容:**)
- **删除的内容:** level of
- **删除的内容:** at
- **删除的内容:** the
- **删除的内容:** (also
- **删除的内容:**)
- **删除的内容:** (in colder seasons mapping is usually influenced by snow cover, lake ice or cloud)
- **删除的内容:** e current
- **删除的内容:** concentrated
- **删除的内容:** Nine orthorectified Landsat TM or ETM+ images were used in this study to map the boundary of supraglacial lakes on eight selected glaciers (indicated in Fig. 1)
- **删除的内容:** The Landsat images, spanning the period from 1990 to 2011 with the same footprint, were selected and downloaded from the Landsat archive of the United State Geological Survey (USGS) based on the following criteria: (1) the lowermost part of the glaciers was (almost) cloud free or and not (or only minimal) covered by snow; (2) the image was acquired during the summer (July to September).

Table 1 List of Landsat images used in this study.

Image ID (File name)	Sensors	Spatial Resolution (m)	Acquisition Date (yyyy-mm-dd)
ETP147r31_5t19900910	TM	28.5	1990-09-10
LE71470311999238SGS00	ETM+	15	1999-08-26
LE71470312002230SGS00	ETM+	15	2002-08-18
LE71470312005222PFS00	ETM+	15	2005-08-10
LT51470312006249IKR00	TM	30	2006-09-06
LT51470312007236IKR00	TM	30	2007-08-24
LT51470312009273IKR01	TM	30	2009-09-30
LT51470312010228IKR01	TM	30	2010-08-16
LT51470312011231KHC01	TM	30	2011-08-19

From the Landsat images, supraglacial lakes are obviously identified on the eight glaciers in the KTTM region. Of all glaciers with lake measurements, seven are the top 7 biggest ones (area > 100 km^2) in the region and the Koxkar Glacier (86.9 km^2) is the most highly debris covered (24.6%) and also a well monitored glacier. The boundaries of these glaciers was manually adapted from the latest GLIMS dataset (Armstrong et al., 2012), based on a Landsat TM image acquired on 24 August 2007. A threshold algorithm on the Normalized Difference Snow Index (TM2-TM5)/(TM2+TM5) of Landsat bands was applied to differentiate clean ice and snow inside the refined boundaries of glaciers. At the same time, the extent of debris-covered area of each glacier was also determined.

To efficiently map supraglacial lakes, we first created a mask which includes all supraglacial lakes or marginal lakes (Figure 3a). Outlines of the supraglacial lakes and marginal lakes were semi-automatically extracted from Landsat image in each year using the ENVI object-based Feature Extraction Module (IDL, 2008). Its workflow consists of two primary steps: find objects and extract features. By adjusting parameters for the scale level and merge level, the procedure is interactively performed to observe whether the lakes boundaries are well delineated or not (Figure 3b). We used this procedure to generate polygon shape files, where the combination of segments finally occupies the whole masked region (Figure 3c). These polygons were then overlaid on the source Landsat image and modified visually by keeping the polygons of lakes only and merge the connected polygons to one lake (Figure 3d). For most Landsat images used, the spatial resolution is about 30 m which requires an area threshold of 3600 m^2 on the final mapping results for the analysis of the supraglacial lakes distribution and changes (Gardelle et al., 2011;Wessels et al., 2002). The uncertainty in the measurement of the lake area was estimated by assuming an error of ± 0.5 pixel on the outlines of the shape (Salerno et al., 2012;Fujita et al., 2009).

删除的内容: By checking carefully on the Landsat images, we found that s

删除的内容: S

删除的内容: of these glaciers

删除的内容: extent

删除的内容: After the glaciers outlines were delineated, clean ice and snow inside the boundary of glaciers was extracted from the image using a band ratio method, which applied a

删除的内容: .
Figure 3 Outlines of the selected glaciers (grey line), debris-covered area (grey fill) and the central flow lines (dashed red line); a shape file (purple) was used for masking the lower region of each glacier for glacial lakes mapping. The results of the 12 September 1990 and 11 August 2005 lake mapping are presented as points of lakes center; lower right inset is a plot of glacier surface profiles along the central flow lines.

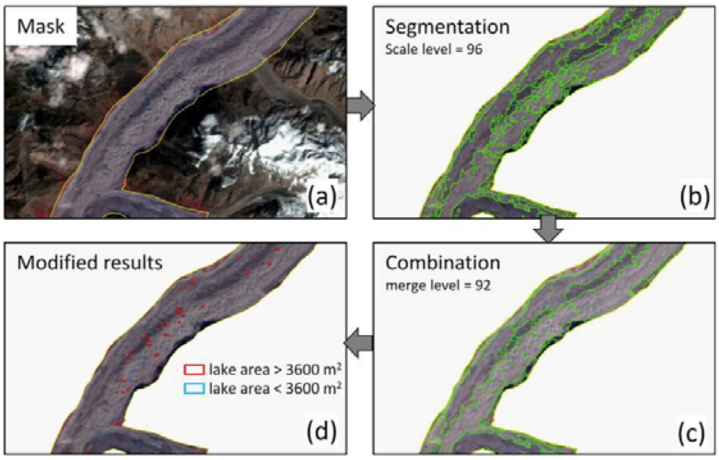

Figure 3 Example of the supraglacial lakes mapping in the lower region of the Tomur Glacier showing the workflow of the lake extraction procedure. Background is the band combination of 432 for a Landsat TM image acquired on 24 August 2007.

In order to exploit the geomorphological characteristics of the glaciers and lakes, we also applied the Shuttle Radar Topography Mission (SRTM V4) digital elevation model (DEM) of 90 m horizontal resolution (http://srtm.csi.cgiar.org/) that has been void filled (Jarvis et al., 2008;Reuter et al., 2007) to demonstrate the hypsography of lakes and glaciers. Since changes of the glacier surface elevation were not remarkable in this region between 1999 and 2009 (-0.23 ± 0.19 m w.e.a^{-1}) (Pieczonka et al., 2013), we assume that, for the statistics on area-elevation distributions of glaciers and supraglacial lakes for each 100 m altitude zone, potential variations of the surface elevation could be neglected. We also ignored the accompanied uncertainty in the calculation of glacier surface gradients since the calculated surface gradient is based on the relative values between DEM pixels (Quincey et al., 2007) .

4 Results

4.1 Glaciers and supraglacial lakes distribution

The 8 selected glaciers, with a total area of 2101.8 km^2, account for about 51% of the area of all glaciers (about 4093 km^2) in the KTTM region. These glaciers distributed from 2689 m a.s.l. to 7053 m a.s.l. Debris cover in the lower part of these glaciers occupies about 17.2% of the total glacier area. On the eight glaciers, we totally mapped 775 supraglacial lakes and 38 marginal lakes. Figure 4 show their distributions and lake size was classified into the 3 categories of lake size (<0.01 km^2, 0.01-0.02 km^2 and >0.02 km^2). The accumulation areas are always steep while the ablation areas are normally gentle when examining the surface slopes along their central flow lines (Figure 4). On average, the slope of the upstream part of the glaciers is ~42.1° and that in the lower part is ~8.9°. Both, the debris cover and the observed supraglacial lakes are located in the lower downstream part of the glaciers.

删除的内容: for

删除的内容: y are span

删除的内容: ning

删除的内容: plotted all

删除的内容: ,

删除的内容: , on the map of the eight investigated glaciers

删除的内容: Debris cover in the lower part of these glaciers occupies about 17.2% of the total glacier area. There exist general morphological features common to all glaciers.

删除的内容: For example, t

删除的内容: 3

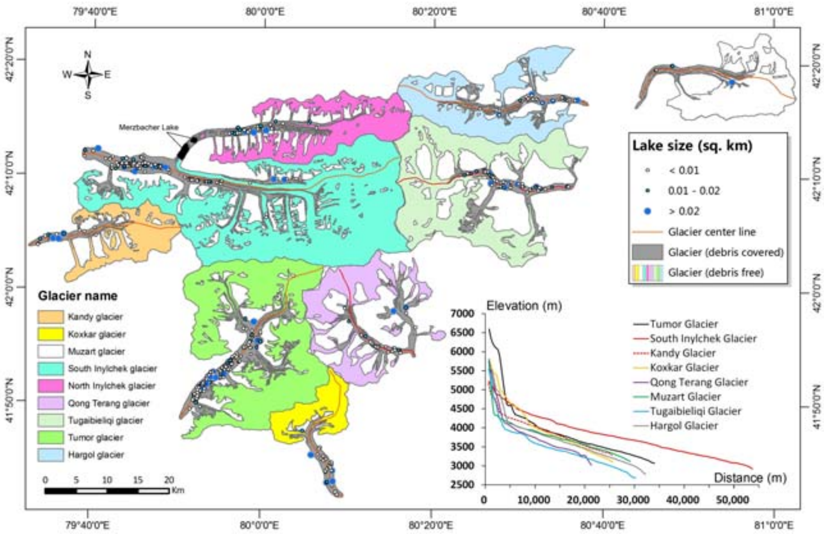

Figure 4 Map of the selected glaciers (debris-free area coloured and debris-covered area grey filled) and their central flow lines (red line), overlaid by all mapped location points of lakes; lower right inset is a plot of glacier surface profiles along the central flow lines.

The majority of supraglacial lakes were located on the Tomur Glacier (TG) and the South Inylchek Glacier (SIG), the two largest debris covered glaciers in the KTTM region. Total area of the supraglacial lakes on TG and SIG occupied from 43.9% (in 1990) to 72.6% (in 2005) of all mapped lakes in the KTTM region. In general, the total area of supraglacial lakes on the TG is larger than the SIG. The SIG is the largest glacier in the KTTM region, 607.13 km^2 in area and 53.7 km in length. Part of its lower branch is calving into the Merzbacher Lake, an ice dammed lake located between the south and north Inylchek Glaciers, with a maximum area of about 4 km^2. The Merzbacher Lake will not be included in our discussion since its size is far out of the range of most glacial lakes investigated in this region and, actually, few Landsat images used here have ever captured the lake when it is filled. The statistics of all mapped supraglacial lakes (the Lake Merzbacher excluded) are presented in Table 2.

Table 2 Geomorphological characteristics of the eight selected glaciers, their debris-covered region and the 1990's and 2005's supraglacial lakes.

Glacier name	Glacier			Debris			Supraglacial lake in **1990**		Supraglacial lake in **2005**	
	Area (km^2)	Length (km)	Elevations (m, a.s.l.)	Area (km^2)	Percentage (%)	Elevations (m, a.s.l.)	Count	Total Area (km^2)	Count	Total Area (km^2)
Tomor Glacier	419.3	36.3	2754-6979	73.7	17.6	2754-4732	31	0.396±0.031	40	0.328±0.031
South Inylcheck Glacier	607.1	53.7	2895-7053	85.4	14.1	2895-4697	21	0.175±0.016	17	0.115±0.012
Kandy Glacier	118.7	25.5	3231-5654	16.0	13.5	3231-4130	7	0.069±0.006	3	0.017±0.002
Koxkar Glacier	86.9	25.6	3016-6037	21.4	24.6	3016-4244	6	0.128±0.008	1	0.008±0.001
Qong Terang Glacier	171.6	21.3	3026-7009	41.7	24.3	3026-4783	8	0.067±0.006	6	0.052±0.005
Tugaibieliqi Glacier	315.4	30.3	2689-6794	44.7	14.2	2689-5110	22	0.333±0.025	8	0.074±0.007
Hargol Glacier	211.4	32.2	2774-6457	37.3	17.6	2774-4923	8	0.131±0.009	2	0.016±0.002
Muzart Glacier	165.8	29.2	2763-6289	22.4	13.5	2763-4345	—	—	—	—
Total	2101.8	—	2489-7053	342.6	17.2	2689-5110	103	1.299±0.103	77	0.610±0.059

删除的内容: .
Since w

删除的内容: e observed that t

删除的内容: , the detailed statistical results of these two glaciers are presented here

删除的内容: , with a slightly larger percentage in numbers from 50% to 74%, respectively

删除的内容: . The Merzbacher Lake

删除的内容: ,

删除的内容: It is the origin of periodical outburst floods at least once every summer since the early 1900s (Glazirin, 2010;Mayer et al., 2008;Ng and Liu, 2009).

删除的内容: is

删除的内容: l

删除的内容: supra

删除的内容: .

Figure 5 displays the distribution of the supraglacial lakes area (as the mean value of all years) with elevation, compared to the area-altitude distribution of debris-free and debris-covered area for total of eight glaciers, TG and SIG separately. Most of the debris-free glacier surface occurs above 4000 m a.s.l. (90.1%) and reaches its maximum at about 4750 m a.s.l. On the other hands, most the debris-covered area is distributed below 4000 m a.s.l. (89.1%) and reaches its maximum at about 3750 m a.s.l. Supraglacial lakes (for area > 3600 m^2) can be found at as high as 3850 m a.s.l, about 800 m lower than the upper boundary of surface debris (4650 m a.s.l.). The largest portion of supraglacial lakes concentrated at about 3250 m a.s.l., below which nearly no clean ice is observed. Therefore, these results indicate that the supraglacial lakes appear at the elevation of the maximum debris cover area, and the lake area reaches a maximum coinciding with the disappearance of debris-free ice.

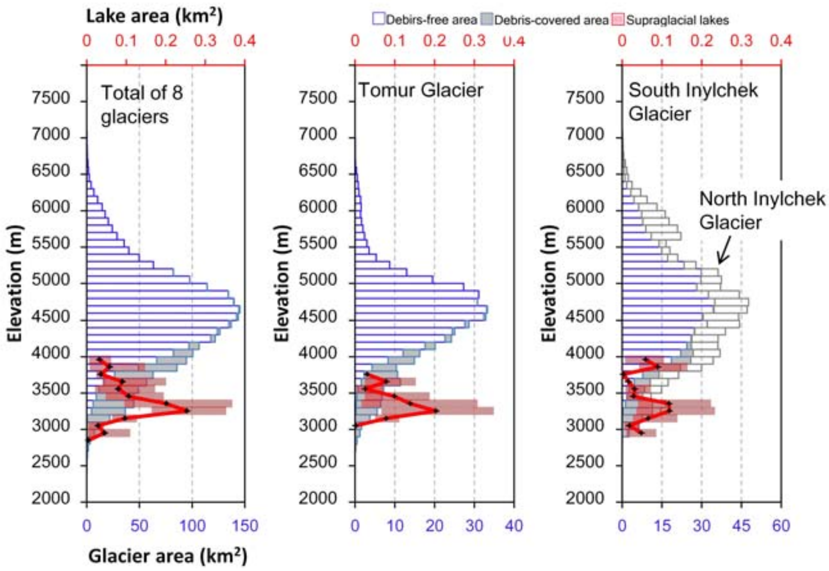

Figure 5 Altitudinal distributions of debris-free area, debris-covered area and supraglacial lakes area (bold red lines show the mean value and light red bars indicate the boundary of minimum and maximum lake areas between 1990 and 2011) for the selected eight glaciers in the KTTM, the TG and the SIG (note the North Inylchek Glacier is also plotted for comparison).

4.2 Multi-year variations of supraglacial lakes

Few studies have systematically investigated the temporal variations of supraglacial lakes considering their total area in a mountain region or on a specific glacier (Salerno et al., 2012;Gardelle et al., 2011). Based on the lakes mapping results, the total and mean areas of supraglacial lakes for the TG, the SIG and the whole KTTM during 1990-2011 summers are given in Figure 6 and their statistics is shown in Table 3. The Landsat images used here are all acquired between August and September. Therefore our results represent a general late summer condition of lake evolution. Over the study period, for the whole KTTM region, the total area of supraglacial lakes varied between 0.628 ± 0.063 km^2 in 2005 and 1.400 ± 0.224 km^2 in 1990, with a mean value of 0.918 ± 0.149 km^2. Figure 6 and Table 3 show that supraglacial lakes did not display a general trend of change but obvious variability either in total area or the mean. During 1990-2011,

删除的内容: .

删除的内容: During 1990-2011, the summer 1990 shows the largest total area of supraglacial lakes while the summer 2005 shows the minimum. Total area of the supraglacial lakes on TG and SIG occupied from 43.9% (in 1990) to 72.6% (in 2005) of all mapped lakes in the KTTM region ... [6]

删除的内容: clean ice

删除的内容: all

删除的内容: and

删除的内容: For these glaciers, m

删除的内容: clean

删除的内容: ice

带格式的: 上标

删除的内容: est elevation

删除的内容: of

删除的内容: which is

删除的内容: eter

删除的内容: S

删除的内容: reach their maximum ... [7]

删除的内容: , for the studied glaciers ... [8]

删除的内容: in

删除的内容: region

删除的内容: closest to the

删除的内容: debris cover area ... [9]

删除的内容: clean

删除的内容: blod

删除的内容: Based on the lakes ... [10]

删除的内容:

删除的内容: with one and a half ... [11]

删除的内容: they

删除的内容: All the statistical data is ... [12]

删除的内容: there was no general ... [13]

the summer 1990 have seen the largest total area of supraglacial lakes while the summer 2005 the minimum (see Table 2), for example, the total area of supraglacial lakes in the whole region varied between 0.628 ± 0.063 km2 in 2005 and 1.400 ± 0.224 km2 in 1990, with a mean value of 0.918 ± 0.149 km2. The total lake area demonstrates a decreased trend between 1990 and 2005 and an expansion during 2005 and 2011. This phenomenon is the same on the TG and the SIG since lakes on the two glaciers dominate the totals of the whole region.

删除的内容: During 1990-2011, the summer 1990 shows the largest total area of supraglacial lakes while the summer 2005 shows the minimum. Supraglacial lakes mapped in 1990 and 2005 are listed in Table 2. Total area of supraglacial lakes in summer of 1990 was more than twofold larger than in 2005. Between 1990 and 2005, the total area of supraglacial lakes showed large fluctuations. In the more recent years, between 2005 and 2011, however, the total area of supraglacial lakes experienced an expanding trend. This trend is also seen on the TG and the SIG, although there existed several heterogeneous periods of expansion or shrinkage.

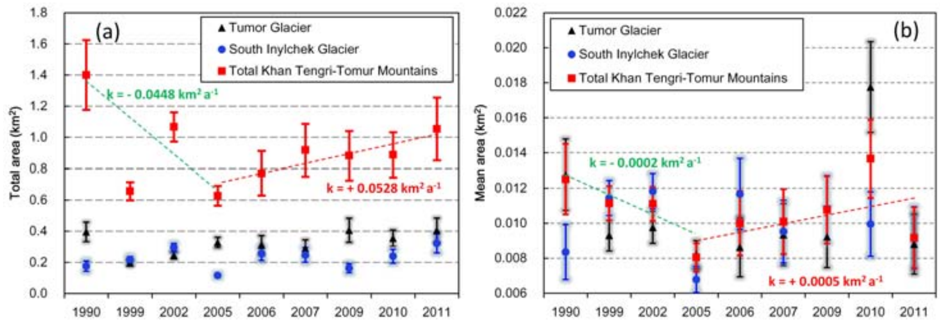

Figure 6 Temporal variation of total (a) and mean (b) area of supraglacial lakes for the total KTTM, the TG and the SIG, between 1990 and 2011. Note trend lines are ploted for the variation of lakes' total area in the whole KTTM region before and after 2005.

Table 3 Total and mean area of the supraglacial lakes during the investigated period.

Image Date	Pixel Size (m)	Lakes of the Tomur Glacier			Lakes of the South Inylchek Glacier			Lakes of the whole KTTM Glacier		
		Total Area	Mean Area	Count	Total Area	Mean Area	Count	Total Area	Mean Area	Count
1990-9-10	28.5	0.396±0.063	0.013±0.002	31	0.176±0.033	0.008±0.002	21	1.400±0.224	0.013±0.002	112
1999-8-26	15	0.195±0.019	0.009±0.001	21	0.217±0.019	0.011±0.001	19	0.657±0.058	0.011±0.001	59
2002-8-18	15	0.244±0.023	0.010±0.001	25	0.296±0.025	0.012±0.001	25	1.066±0.094	0.011±0.001	96
2005-8-10	15	0.328±0.033	0.008±0.001	40	0.115±0.012	0.007±0.001	17	0.628±0.063	0.008±0.001	78
2006-9-06	30	0.311±0.061	0.009±0.002	36	0.257±0.044	0.012±0.002	22	0.770±0.142	0.010±0.002	77
2007-8-24	30	0.289±0.055	0.009±0.002	31	0.248±0.047	0.010±0.002	26	0.918±0.169	0.010±0.002	91
2009-9-30	30	0.406±0.077	0.009±0.002	44	0.162±0.029	0.011±0.002	15	0.883±0.158	0.011±0.002	82
2010-8-16	30	0.355±0.052	0.018±0.003	20	0.239±0.044	0.010±0.002	24	0.888±0.144	0.014±0.002	65
2011-8-19	30	0.405±0.079	0.009±0.002	46	0.322±0.061	0.010±0.002	35	1.054±0.201	0.009±0.002	115
Mean	—	**0.322±0.051**	**0.010±0.002**	**33**	**0.234±0.038**	**0.010±0.002**	**23**	**0.918±0.149**	**0.011±0.002**	**86**

The variation of the annual mean area of supraglacial lakes is presented in Figure 6b. Supraglacial lakes on the TG and the SIG generally expanded in this period, although the mean area shows a large variability. The mean area of all investigated supraglacial lakes varied between 0.007 ± 0.001 km^2 (for the SIG in 2005) and 0.018 ± 0.002 km^2 (for the TG in 2010). For both the KTTM region and the two glaciers, the averaged multi years mean area of supraglacial lakes is close to the same value (0.010 ± 0.002 km^2, Table 3). The minimum mean area of supraglacial lakes in the KTTM region also occurred in 2005 (0.008 ± 0.001 km^2), while the maximum mean area occurred in 2010 and then in 1990. For the whole KTTM and the TG, the mean supraglacial lake area showed a transient maximum in 2010 after the gradual increase between 2005 and 2010

删除的内容: , for the whole KTTM the value is 0.011 ± 0.002 km^2, and then decreased again to the mean size of 0.009 ± 0.002 km^2 in 2011. Since the mean lake size changed only on a moderate scale, the year-to-year fluctuation of the lake numbers is an important parameter to determine the total area variation. For example the growth of total area of supraglacial lakes in summer of 2011 displayed in Figure 6a was governed by the increase of lake numbers.

For different area classes of supraglacial lakes, their year-by-year variations of number and total area show in Figure 7. The number of smaller supraglacial lakes (area < 0.02 km^2) is by far larger than the bigger lakes (area > 0.02 km^2). On the average between 1990 and 2011, the numbers of supraglacial lakes were 60, 17 and 9 for areas <0.01 km^2, 0.01 km²-0.02 km^2 and >0.02 km^2, respectively. The total area of supraglacial lakes for the 3 area classes, however, contributed nearly equally to the overall lakes area of the individual year, with mean values of 0.36 km^2, 0.23 km^2 and 0.32 km^2 for the different area classes. Generally, larger supraglacial lakes show more remarkable variations in area than smaller ones. Standard deviations (SD) for total area of these three size classes of supraglacial lakes are 0.0098 (areas <0.01 km^2), 0.0035 (0.01 km²<area<0.02 km^2) and 0.0256 (area > 0.02 km^2). It is indicated that multi-year variation of total area was dominated by those larger supraglacial lakes. As a consequence, the year-by-year fluctuations are similar between total area (Figure 6a) and area of larger lakes (Figure 7). It is also obvious that the anomalies of the total area which occurred in 1990, 2002 and 2005 were predominant due to the area changes of larger supraglacial lakes (Figure 7, right panel). In 2010, the total area of larger supraglacial lakes (area>0.02 km^2) was more than double of those smaller lakes (area<0.01km^2), therefore the calculated mean lake area in 2010 (Figure 6b) was the highest.

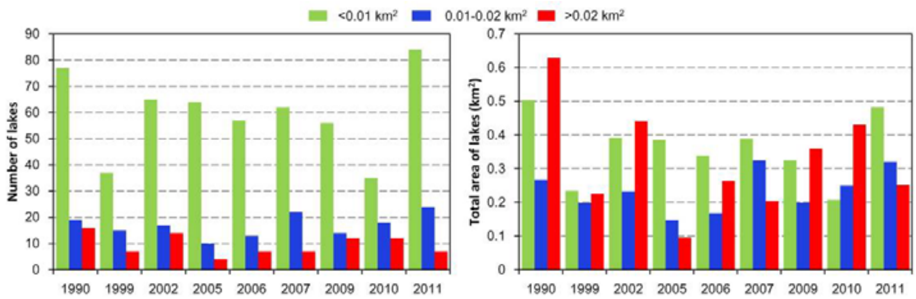

Figure 7 Changes of numbers (left) and total area (right) for three area classes of supraglacial lakes between 1990 and 2011.

5 Discussions

5.1 Glacio-geomorphological control on the supraglacial lake distribution

All mapped supraglacial lakes in the KTTM region are detected in the lower flat downstream part of the investigated glaciers. Their locations and sizes show remarkable fluctuations year by year. This flatter part of the glaciers (with a mean slope of 8.9°) is also the region where extensive debris-cover exists in (Figure 4). The formation and existence of supraglacial lakes is strongly related to the local surface slope (Sakai and Fujita, 2010). According to Reynolds (2000), at a surface gradient less than 10° supraglacial lakes can form and potentially exist for longer duration. Following the classification by Reynolds (2000) and Bolch et al. (2008), glacier surface slope was divided into 5 classes based on the SRTM DEM (Figure 8). As mentioned by Bolch et al. (2008), lake areas in the elevation model also contain short steep slopes of ice cliffs around the

删除的内容: .
During the 9 years period between 1990 and 2011, a total of 775 supraglacial lakes in the KTTM region were mapped, with an annual mean number of 86. The annual mean number of supraglacial lakes on the TG and SIG were 33 (38.4%) and 23 (26.7%), respectively.

删除的内容: also

删除的内容: different

删除的内容: 01

删除的内容: 01

删除的内容: between

删除的内容: and

删除的内容: lakes

删除的内容: .

删除的内容: .

删除的内容: .

带格式的: 上标

带格式的: 上标

删除的内容: **formation, expansion and drainage**

删除的内容: 3 and Figure 7

删除的内容: some

删除的内容: The formation of larger supraglacial lakes can occur where surface gradients range between 0-2°. In Figure 9, we plotted all mapped 775 supraglacial lakes and 38 marginal lakes, classified into the 3 categories of lake size (<0.01 km^2, 0.01-0.02 km^2 and >0.02 km^2), on the surface gradient map of the eight investigated glaciers.

supraglacial lakes or ponds. Therefore, to reduce the noise induced by ice cliffs, the slope relating to a supraglacial lake was calculated from the value of adjacent DEM cells nearby the center of the lake using bilinear interpolation.

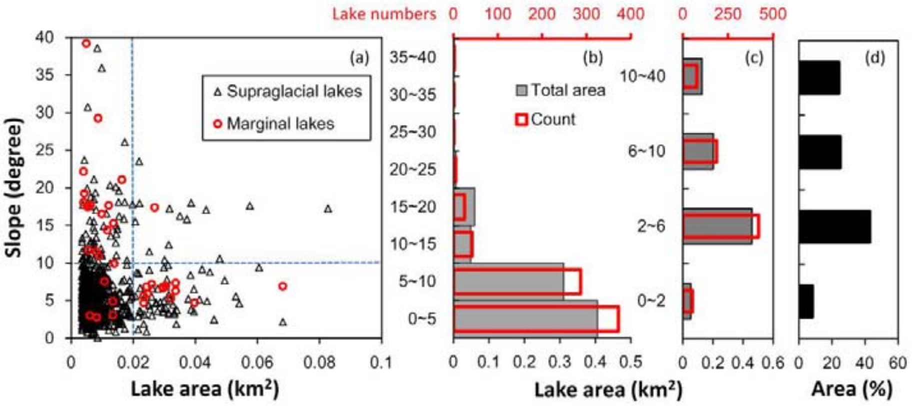

Figure 8 (a), (b) and (c) Slope distributions of 775 supraglacial lakes and 38 marginal lakes mapped between 1990 and 2011 in the Khan Tengri-Tomur Mountains; (d) Frequency distribution of the surface slope of the entire debris-covered area of the 8 glaciers.

Figure 8 shows the calculated surface slopes plotted against the lakes area. It is obvious that most large lakes (71 of 86 lakes with area > 0.02 km^2) are located in the region with surface gradients less than 10°. In the same way, for the 689 supraglacial lakes with an area less than 0.02 km^2, 608 of them are located in the region with surface gradient less then 10°. As expected, both the total area and the numbers of supraglacial lakes show a decrease with increasing surface slope. The annual mean total area of supraglacial lakes located in regions of less than 10° surface gradient accounts for 85.7% of the total. The statistic based on the classification suggested by Reynolds (2000), however, indicates that large portion of lake area in the KTTM is distributed in the regions with surface gradient between 2° and 6° but not the value less than 2° suggested by Reynolds (2000). This similar fact could also be detected in the Figure 5 in Bolch et al. (2008). These could be explained by the frequency distribution of surface slope of the entire debris-covered area (Figure 8d). Since the area of surface gradient between 2° and 6° accounts for the majority portion (42.8%) in the lower ablation zone of these glaciers and it is also very favorable for the development of supraglacial lakes, lake area reaching its maximum in these regions is natural.

We did not extract the surface velocity of investigated glaciers, although the flow velocity of a glacier is inherently related to its surface slope (Paterson, 1994). Further investigations are needed for depicting the region-wide spatial distribution pattern of glacier surface velocity fields, which may play a more direct role in controlling the existence and lifespan of a supraglacial lake (Benn et al., 2012;Bolch et al., 2008). Surface flow fields of individual glaciers may help to illustrate the possible reasons for the infrequent existence of supraglacial lakes on the surface of some glaciers, such as the Muzart Glacier (given the similar patterns of debris-cover, surface gradients and relative lower ice tongue); and analyzing multi-year changes of velocity may also contribute to the explanation of the supraglacial lake year-to-year fluctuations.

In the KTTM region, no moraine dammed glacial lake was found until present time, in

删除的内容: '

删除的内容: s

contrast to the large number detected on debris-covered glaciers in the Himalaya (Richardson and Reynolds, 2000;Komori, 2008), the southern Alps (Warren and Kirkbride, 2003;Kirkbride and Warren, 1999) and the Patagonian Andes (Dussaillant et al., 2009;Reynolds, 1992). It has been confirmed that most of these reported moraine dammed lakes are a result of the expanding and merging of supraglacial lakes that periodically fill up on the surface of extensive debris-covered parts of glaciers (Reynolds, 2000). In the lower part of the dendritic-type glaciers in the KTTM, we have identified some regions where supraglacial lakes are likely to develop (Figure 8). These regions are prone to coalesce and growth of supraglacial lakes, e.g., in the Himalayas (Benn et al., 2012) and South Alps (Kirkbride and Warren, 1999), lending the potential for larger lake development. Actually, from results of the current investigation, most supraglacial lakes with an area larger than 0.02 km^2 are also located in the same regions. Regarding water storage, flood hazards and also the influence of lakes on the glacier characteristics and dynamics, these water bodies with larger areas are much more important than the small ones.

5.2 Relationship between supraglacial lakes variation and climatic conditions in summer and spring

The size of supraglacial lakes varies with the lake water balance. Once a supraglacial lake forms, it will grow rapidly due to several coupled physical mechanisms leading to enhanced ice melt around and on the subaqueous interface of the lake (Reynolds, 2000;Benn et al., 2001;Benn et al., 2000). Generally, sources of lake water include (1) melting of ice around the lake and within the lake itself, (2) melt water transported through englacial channels or inflow from supraglacial streams and (3) water directly supplied by rainfall or snow melt. The growth of a supraglacial lake will be balanced by a combination of lake water loss via outflow and evaporation. Continuous lateral calving and melt at the water-line and subsurface down-cutting may lead to abrupt drainage of the lake, when encountering an ice crevasse or englacial channels (Fountain and Walder, 1998;Irvine-Fynn et al., 2011). Repeated observations of supraglacial lakes on the Ngozumpa Glacier in the Khumbu Himalaya (Benn et al., 2001) and also on the Koxkar Glacier during our 2010 expedition indicate the existence of connections between supraglacial lakes and glacial drainage systems before the lake drainage. Sometimes the activation of this connection is due to ice motions, which may open a pathway for lake water drainage (Das et al., 2008;van der Veen, 2007).

We assume perennial supralglacial lakes reach their yearly maximum in the late summer since intensive water input happens due to precipitation and ablation in the same season. Those temporal lakes may drain out their water due to the weak capacity for more water input in the summer. Therefore, the total and mean areas of all supraglacial lakes may have something to do with climate changes. Considering that the state of supraglacial lakes in summer is influenced by both summer and pre-summer conditions, we therefore discuss here their relationships with total precipitation and mean air temperature over summer (July to September) and spring (April to June) for each specific year. We extracted spring and summer climatic conditions (Figure 9) of the Tianshan Station in Kyrgyz for analysis, since it located closely to our study region (Figure 1).

删除的内容: 3

删除的内容: As previously mentioned, supraglacial lakes are highly variable in space and time.

删除的内容: During winter time, lakes either disappear (due to the lack of water input), or freeze over.

删除的内容: Ignoring the glacial surface topographic changes, the lake evolution will be primarily affected by the climatic variations.

删除的内容: are

删除的内容: extracted

删除的内容: from

删除的内容: monthly

删除的内容: data

删除的内容: (Figure 13)

删除的内容: Between 1990 and 2011, the variation of total precipitation over the two seasons is remarkable. For example precipitation over the ablation season in 1990 was peculiarly higher (about 5 times) than in 2005 or 2006. For air temperature, its summer mean values show less fluctuation than during spring, which dominate the multi-year variations of mean air temperature for the whole ablation season between 1990 and 2011.

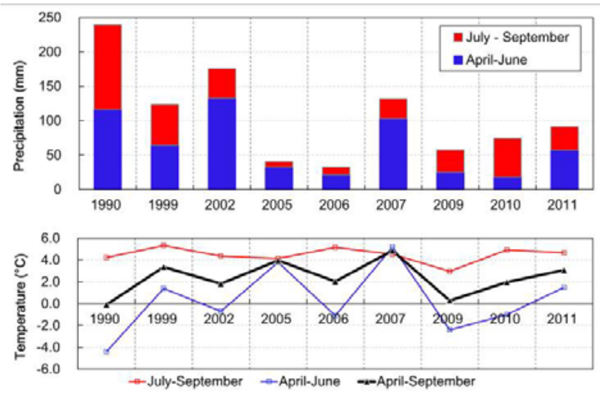

Figure 9 Total precipitation and mean air temperature over summer (July to September) and spring (April to June) of each specific year at the Tianshan Station.

By comparing the climatic fluctuations with the variations of supraglacial lakes (Figure 10), we found that the area of supraglacial lakes was positively correlated with precipitation, while correlation was negative with respect to the mean air temperature. Since liquid precipitation acts as the direct input of liquid water into the supraglacial lakes, its total amount over summer is positively correlated to the area of supraglacial lakes. Air temperature increase, however, has a dual function in the development of supraglacial lakes: more melt water enlarges the supraglacial lakes due to enhanced ablation and, on the other hand, it may accelerate the drainage of lakes by promoting the development of glacial drainage systems from unconnected to connected structures (Irvine-Fynn et al., 2011). In some years, such as in 1990, the drainage of supraglacial lakes is likely to be limited by the relatively cool ablation season whereas a superimposed precipitation (if snow then it will melt soon during the ablation season) contributes water input to the lake expansions. In 2005, in contrast, little precipitation (especially over summer) together with a warmer ablation season could explain the observations of the minimum total and mean area of supraglacial lakes in that summer.

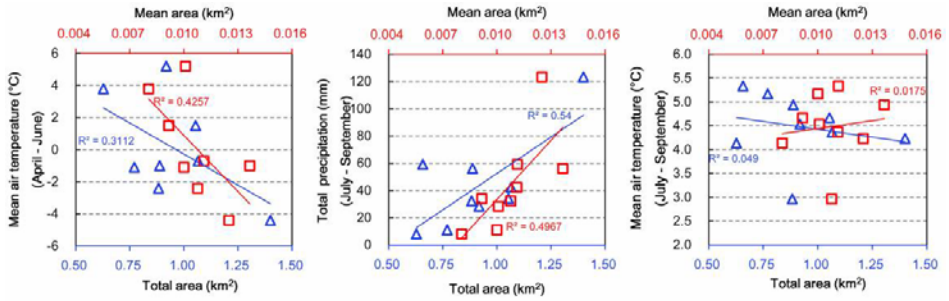

Figure 10 Correlations between supraglacial lake area (blue triangle: total area; red square: mean area) and climatic conditions (Tianshan Station) in summer (July to September) and spring (April to June).

An obviously negative correlation between supraglacial lakes area and mean air temperature for spring (April to June) but not for summer (July to September) likely indicates that most connected drainage systems have been developed between April and June. The development of glacial drainage systems leads to some drainage of supraglacial lakes, resulting in the lakes total area shrinkage. The mean area of supraglacial lakes also decreased with the increase of mean air temperature during spring. This likely indicates that more drainage events happened to larger supraglacial lakes, which could have induced a general decrease of mean lake area. This could also be confirmed by Figure 7 that, in the summer of 2005, the remarkable shrinkage (both the numbers and their total area) of larger supraglacial lakes contributed to the major variations, whereas no remarkable changes happened to the smaller lakes.

6 Conclusions

We presented the distribution and multi-year variations of supraglacial lakes for several selected glaciers around the KTTM region, the largest glacierized mountain range in the Tianshan. A total of 775 supraglacial lakes and 38 marginal glacial lakes (minimum size 3600 m²) were mapped on Landsat images in the period 1990 to 2011. This relates to a mean of 86 lakes occurring each year on these glaciers. The distribution of all mapped supraglacial lakes shows that supraglacial lakes in the KTTM region initially appear at about 3850 m a.s.l., about 800 meter lower than the debris cover emergence (4650 m a.s.l.), and reach their maximum area at about 3250 m a.s.l., the altitude where bare ice disappears entirely. For the whole KTTM region, the total area of supraglacial lakes varied between 0.628 ± 0.063 km^2 in 2005 and 1.400 ± 0.224 km^2 in 1990, with a mean value of 0.918 ± 0.149 km^2. The total area of supraglacial lakes showed large fluctuations between 1990 and 2005 whereas in recent years, between 2005 and 2011, experienced an expanding trend. Mean area of supraglacial lakes showed a transient maximum in 2010 after the expanding between 2005 and 2010 and then decreased to the mean size scale of 0.009 ± 0.002 km^2 in 2011. The area of supraglacial lakes was positively correlated with the total precipitation in summer (July to September) while correlated negatively to the mean air temperature over pre-summer (April to June). Air temperature fluctuations during the pre-summer likely have more impact on the different evolution proceedings of the development of glacial drainage from unconnected to connected systems, which may lead to the drainage of some larger supraglacial lakes and resulted in shrinkage of the total and mean lakes area over the summer seasons.

The majority of the investigated supraglacial lakes were located on the surface of the Tomur Glacier and the South Inylchek Glacier, two typical debris-covered dendritic-type glaciers in the KTTM region. The total area of supraglacial lakes on the surface of TG and SIG occupied 43.9% (in 1990) to 72.6% (in 2005) of all mapped lakes in the KTTM regions, and accounted for 50% to 74% in numbers, respectively. Some regions in the lower part of the TG and SIG are found more favorable for the supraglacial lakes development. Future coalescing and growth of these supraglacial lakes will lead to the development of larger lake on lower part of the glaciers. A continued monitoring is necessary to assess the future evolution of supraglacial lakes in the KTTM region.

Acknowledgements

Thank M. Pelto and two anonymous reviewers for their comments on the improvement of the manuscript. Our work was initiated from the Chinese-German collaborative field expedition at the Koxkar Glacier in the Tomur Mountains, partly funded by the Deutsche Forschungsgemeinschaft (DFG fund MA 3347/4). Thanks to Han Haidong, Wang Xin, Martin Juen and Elisabeth Mayr for the field assistance. This work was funded by the National Science and Technology Support

Program of Chinese MOST (Grant No. 2012BAC19B07 and 2013BAC10B01), the National Natural Science Foundation of China (Grant No. 41190080, 41371094) and a DAAD research-stay funding award (A-12-00042). The work was also supported by the Fund of State Key Laboratory of Cryosphere Sciences (Grant No. SKLCS 2011-10).

References

Aizen, V. B., Aizen, E. M., Dozier, J., Melack, J. M., Sexton, D. D., and Nesterov, V. N.: Glacial regime of the highest Tien Shan mountain, Pobeda-Khan Tengry massif, Journal of Glaciology, 43, 503-512, 1997.

Armstrong, R., Raup, B., Khalsa, S. J. S., Barry, R., Kargel, J., Helm, C., and Kieffer, H.: GLIMS glacier database. Boulder, Colorado USA:National Snow and Ice Data Center. Digital media., 2012.

Bajracharya, B., Shrestha, A. B., and Rajbhandari, L.: Glacial lake outburst floods in the Sagarmatha region - Hazard assessment using GIS and hydrodynamic modeling, Mountain Research and Development, 27, 336-344, 10.1659/mrd.0783, 2007.

Benn, D., Benn, T., Hands, K., Gulley, J., Luckman, A., Nicholson, L., Quincey, D., Thompson, S., Toumi, R., and Wiseman, S.: Response of debris-covered glaciers in the Mount Everest region to recent warming, and implications for outburst flood hazards, Earth-Science Reviews, 114, 156-174, 2012.

Benn, D. I., Wiseman, S., and Warren, C. R.: Rapid growth of a supraglacial lake, Ngozumpa Glacier, Khumbu Himal, Nepal, Debris-Covered Glaciers, 264, 177-185, 2000.

Benn, D. I., Wiseman, S., and Hands, K. A.: Growth and drainage of supraglacial lakes on debris-mantled Ngozumpa Glacier, Khumbu Himal, Nepal, Journal of Glaciology, 47, 626-638, 2001.

Bolch, T., Buchroithner, M. F., Peters, J., Baessler, M., and Bajracharya, S.: Identification of glacier motion and potentially dangerous glacial lakes in the Mt. Everest region/Nepal using spaceborne imagery, Natural Hazards and Earth System Sciences, 8, 1329-1340, 2008.

Box, J. E., and Ski, K.: Remote sounding of Greenland supraglacial melt lakes: implications for subglacial hydraulics, Journal of Glaciology, 53, 257-265, 2007.

Campbell, W. J., and Rasmussen, L. A.: The production, flow and distribution of melt water in a glacier treated as a porous medium, Hydrology of Glaciers, 11-27, 1973.

Cuffey, K. M., and Paterson, W. S. B.: The Physics of Glaciers, 4th Edition, Elsevier, 2010.

Das, S. B., Joughin, I., Behn, M. D., Howat, I. M., King, M. A., Lizarralde, D., and Bhatia, M. P.: Fracture propagation to the base of the Greenland Ice Sheet during supraglacial lake drainage, Science, 320, 778-781, 10.1126/science.1153360, 2008.

Dussaillant, A., Benito, G., Buytaert, W., Carling, P., Meier, C., and Espinoza, F.: Repeated glacial-lake outburst floods in Patagonia: an increasing hazard?, Nature Hazards, DOI 10.1007/s11069-009-9479-8, 2009.

Fountain, A. G., and Walder, J. S.: Water flow through temperate glaciers, Reviews of Geophysics, 36, 299-328, 1998.

Fujita, K., Sakai, A., Nuimura, T., Yamaguchi, S., and Sharma, R. R.: Recent changes in Imja Glacial Lake and its damming moraine in the Nepal Himalaya revealed by in situ surveys and multi-temporal ASTER imagery, Environmental Research Letters, 4, 1748-9326, 10.1088/1748-9326/4/4/045205, 2009.

Gardelle, J., Arnaud, Y., and Berthier, E.: Contrasted evolution of glacial lakes along the Hindu Kush Himalaya mountain range between 1990 and 2009, Global and Planetary Change, 75, 47-55, doi:10.1016/j.gloplacha.2010.10.003, 2011.

Glazirin, G. E.: A century of investigations on outbursts of the ice-dammed lake Merzbacher (central Tien Shan), Austrian Journal of Earth Sciences, 103, 171-179, 2010.

Hagg, W., Mayer, C., Lambrecht, A., and Helm, A.: Sub-debris melt rates on southern Inylchek Glacier, central Tian Shan, Geografiska Annaler Series a-Physical Geography, 90A, 55-63, 2008.

Han, H., Jian, W., Junfeng, W., and Shiyin, L.: Backwasting rate on debris-covered Koxkar glacier, Tuomuer mountain, China, Journal of Glaciology, 56, 287-296, 2010.

Han, H. D., Ding, Y. J., and Liu, S. Y.: A simple model to estimate ice ablation under a thick debris layer, Journal of Glaciology, 52, 528-536, 2006.

Hock, R.: Glacier melt: a review of processes and their modelling, Progress in Physical Geography, 29, 362-391, Doi 10.1191/0309133305pp453ra, 2005.

ENVI Feature Extraction Module User's Guide, 2008.

Irvine-Fynn, T. D. L., Hodson, A. J., Moorman, B. J., Vatne, G., and Hubbard, A. L.: Polythermal glacier hydrology: a review, Reviews of Geophysics, 49, RG4002, doi:4010.1029/2010RG000350, 2011.

Jain, S. K., Lohani, A. K., Singh, R. D., Chaudhary, A., and Thakural, L. N.: Glacial lakes and glacial lake outburst flood in a Himalayan basin using remote sending and GIS, Natural Hazards, 62, 887-899, doi: 10.1007/s11069-012-0120-x, 2012.

Jansky, B., Engel, Z., Sobr, M., Benes, V., Spacek, K., and Yerokhin, S.: The evolution of Petrov lake and moraine dam rupture risk (Tien-Shan, Kyrgyzstan), Natural Hazards, 50, 83-96, 10.1007/s11069-008-9321-8, 2009.

Jansky, B., Sobr, M., and Engel, Z.: Outburst flood hazard: case studies from the Tien-Shan Mountains, Kyrgyzstan, Limnologica-Ecology and Management of Inland Waters, 40, 358-364, 2010.

Jansson, P., Hock, R., and Schneider, T.: The concept of glacier storage: a review, Journal of Hydrology, 282 116-129, 2003.

Jarvis, A., Reuter, H. I., Nelson, A., and Guevara, E.: Hole-filled seamless SRTM data V4, International Centre for Tropical Agriculture (CIAT), available from http://srtm.csi.cgiar.org., 2008.

Juen, M., Mayer, C., Lambrecht, A., Haidong, H., and Shiyin, L.: Impact of varying debris cover thickness on catchment scale ablation: a case study for Koxkar glacier in the Tien Shan, The Cryosphere Discussions, 7, 5307-5332, doi:10.5194/tcd-7-5307-2013, 2013.

Kirkbride, M. P., and Warren, C. R.: Tasman Glacier, New Zealand: 20th-century thinning and predicted calving retreat, Global and Planetary Change, 22, 11-28, 1999.

Komori, J.: Recent expansions of glacial lakes in the Bhutan Himalayas, Quaternary International, 184, 177-186, 2008.

Mayer, C., Lambrecht, A., Hagg, W., Helm, A., and Scharrer, K.: Post-drainage ice dam response at Lake Merzbacher, Inylchek glacier, Kyrgyzstan, Geografiska Annaler Series a-Physical Geography, 90A, 87-96, 2008.

Mayer, C., Lambrecht, A., Eder, K., Juen, M., and Liu, Q.: Ice cliff ablation derived from high resolution surface models, based on close-range photogrammetry, Geophysical Research Abstracts, 13, EGU2011-11078, 2011.

Ng, F., and Liu, S. Y.: Temporal dynamics of a jökkulhlaup system, Journal of Glaciology, 55, 651-665, 2009.

Paterson, W.: The physics of glaciers (3rd Ed.), Oxford Press, Butterworth-Heinemann, 1994.

Pieczonka, T., Bolch, T., Junfeng, W., and Shiyin, L.: Heterogeneous mass loss of glaciers in the Aksu-Tarim Catchment (Central Tien Shan) revealed by 1976 KH-9 Hexagon and 2009 SPOT-5 stereo imagery, Remote Sensing of Environment, 130, 233-244, 2013.

Quincey, D. J., Richardson, S. D., Luckman, A., Lucas, R. M., Reynolds, J. M., Hambrey, M. J., and Glasser, N. F.: Early recognition of glacial lake hazards in the Himalaya using remote sensing datasets, Global and Planetary Change, 56, 137-152, 10.1016/j.gloplacha.2006.07.013, 2007.

Reuter, H. I., Nelson, A., and Jarvis, A.: An evaluation of void filling interpolation methods for SRTM data, International Journal of Geographical Information Science, 21, 983-1008, 2007.

Reynolds, J. M.: The Identification and Mitigation of Glacier-Related Hazards - Examples from the Cordillera Blanca, Peru, in Geohazards, edited by G. J. H. McCall, et al., 143-157, 1992.

Reynolds, J. M.: On the formation of supraglacial lakes on debris-covered glaciers, IAHS Publication, 153-164, 2000.

Richardson, S. D., and Reynolds, J. M.: An overview of glacial hazards in the Himalayas, Quaternary International, 65-6, 31-47, 2000.

Roberts, M. J.: Jökulhlaups: a reassessment of floodwater flow through glaciers, Reviews of Geophysics, 43, P1-21, 2005.

Sakai, A., Nakawo, M., and Fujita, K.: Melt rate of ice cliffs on the Lirung Glacier, Nepal Himalayas, 1996, Bulletin of Glacier Research, 16, 57-66, 1998.

Sakai, A., Takeuchi, N., Fujita, K., and Nakawo, M.: Role of supraglacial ponds in the ablation process of a debris-covered glacier in the Nepal Himalayas, Debris-Covered Glaciers, 265, 119-130, 2000.

Sakai, A., and Fujita, K.: Formation conditions of supraglacial lakes on debris-covered glaciers in the Himalaya, Journal of Glaciology, 56, 177-181, 2010.

Salerno, F., Thakuri, S., Agata, C. D., Smiraglia, C., Manfredi, E. C., Viviano, G., and Tartari, G.: Glacial lake distribution in the Mount Everest region: Uncertainty of measurement and conditions of formation, Global and Planetary Change, 92-93, 30-39, doi: 10.1016/j.gloplacha.2012.04.001, 2012.

Shi, Y.: Concise glacier inventory of China, Shanghai, Shanghai Popular Science Press, 205pp, 2008.

Thompson, S. S., Benn, D. I., Dennis, K., and Luckman, A.: A rapidly growing moraine-dammed glacial lake on Ngozumpa Glacier, Nepal, Geomorphology, 145-146, 1-11, 2012.

van der Veen, C. J.: Fracture propagation as means of rapidly transferring surface meltwater to the base of glaciers, Geophysical Research Letters, 34, 10.1029/2006gl028385, 2007.

Wang, L., Wenjing, Z., and Zhen, S.: Primary results of the study on modern glaciers in the region of Mt. Tuomuer, Journal of Glaciology and Geocryology, 2, 15-18. (in Chinese with English abstract), 1980.

Wang, X., Shiyin, L., Haidong, H., Jian, W., and Qiao, L.: Thermal regime of a supraglacial lake on the debris-covered Koxkar Glacier, southwest Tianshan, China, Environmental Earth Sciences, 67, 175-183, doi: 10.1007/s12665-011-1490-1, 2011.

Warren, C. R., and Kirkbride, M. P.: Calving speed and climatic sensitivity of New Zealand lake-calving glaciers, Annals of Glaciology, 36, 173-178, 2003.

Wessels, R. L., Kargel, J. S., and Kieffer, H. H.: ASTER measurement of supraglacial lakes in the Mount Everest region of the Himalaya, Annals of Glaciology, 34, 399-408, Doi

10.3189/172756402781817545, 2002.

Figure caption page

List of figures

List of Tables